

Diurnal and Seasonal Changes in Structure of the Mid-Latitude Quiet Ionosphere

J. W. Wright

Contribution from Central Radio Propagation Laboratory, National Bureau of Standards, Boulder, Colo.

(Received December 14, 1961)

Typical examples of $N(h)$ data from a series of NBS publications on ionospheric electron densities are described briefly as an introduction to data available from a one-year's program beginning during the International Geophysical Cooperation, 1959. The entire body of data is then illustrated in compact form, and discussed phenomenologically. In a synthesis and interpretation, it is concluded that diurnal, seasonal, and latitudinal temperature variations in the F region may explain many features of the quiet-day behavior of that region. A corpuscular component of heating at mid and high latitudes is suggested as accounting for the seasonal anomaly in the daytime F region; the anomaly is assigned to the summer season rather than to winter, on the basis of evidence given. The nighttime electron density variations are found to be explainable by the loss rate at the equilibrium height to which the layer drifts under the influence of diffusion. An appendix discusses the day-to-day variability of the data.

1. Introduction

By the end of the IGY, the number of ionospheric soundings reduced to electron density profiles was comparatively small, measured in terms of the very large vertical soundings program then underway. The original difficulties stemmed from the considerable labor necessary for manual computation of single profiles, but by the time of the IGY, the availability of electronic computers had largely eliminated this. The remaining limitation was the rather formidable amount of scaled data necessary for each computation. The IGY electron density profile surveys conducted by Schmerling [1957] and Thomas and Vickers [Thomas, 1959] for selected stations on International Quiet or Regular World Days were limited in their scope by the large amount of data preparation necessary.

When the National Bureau of Standards embarked upon a similar program early in the IGC (1959), part of the effort was devoted to developing techniques by which the valuable manpower resources of the network of U.S. and associated vertical soundings stations—already the mainstay of the conventional ionospheric soundings data published by NBS—could be applied to numerical reduction of their ionograms for $N(h)$ analyses. Simple methods were developed for this purpose, permitting the station scientist to derive and tabulate data for subsequent $N(h)$ analysis by the central laboratory's computer. These methods, applied to the hourly ionograms of a day's observations, require about the same effort as the preparation of a quarter-hourly f -plot.

Since May 1959, the NBS has conducted an hourly electron density profile survey, using data provided by the ionospheric stations, from a current

total of 11 stations. These stations, their affiliation, and their initial date of participation in the program are given in table 1.

Our first objective in the study of these data has been to classify and describe the mean quiet geographical, temporal, and height structure of the northern mid-latitude ionosphere. For this purpose, five of these stations (Newfoundland, Ft. Monmouth, White Sands, Grand Bahama Island, and Puerto Rico) are close enough together geographically to permit the delineation of the structure of the mean quiet ionosphere between geographic latitudes of 15° to 50°N , and geomagnetic latitudes of 30°N to 59°N , with some confidence. The results from these stations for one year of data (March 1959–April 1960) are being issued by the NBS in a series of Technical Notes [Wright et al., 1959–1961]. It is the purpose of this paper to review this considerable volume of data, to portray it in a different summary form, and to discuss certain other results which assist in the interpretation of the whole. Finally there will be given a synthesis and interpretation of the data in the light of contemporary theory.

TABLE 1

Station	Affiliation	Latitude	Longitude	Mag. dip	Began $N(h)$
Puerto Rico.....	NBS.....	$18^\circ 30' \text{ N}$	$67^\circ 12' \text{ W}$	51.5° N	Jan. 1959
Grand Bahama Is...	USA SigC	$26^\circ 40' \text{ N}$	$78^\circ 22' \text{ W}$	59.5° N	Feb. 1959
Fort Monmouth...	USA SigC	$40^\circ 15' \text{ N}$	$74^\circ 01' \text{ W}$	51.7° N	Feb. 1959
White Sands, N.M...	USA SigC	$32^\circ 24' \text{ N}$	$106^\circ 52' \text{ W}$	60° N	Mar. 1959
St. Johns, Nfd.....	DRTE.....	$47^\circ 33' \text{ N}$	$52^\circ 40' \text{ W}$	72° N	June 1959
Adak, Alaska.....	USA SigC	$51^\circ 54' \text{ N}$	$176^\circ 39' \text{ W}$	63° N	June 1959
Okinawa, Ryukus...	USA SigC	$26^\circ 30' \text{ N}$	128° W	36.5° N	June 1959
Thule, Greenland...	USA SigC	$76^\circ 31' \text{ N}$	$68^\circ 50' \text{ W}$	86.2° N	July 1959
Huancayo, Peru.....	NBS.....	$12^\circ 03' \text{ S}$	$75^\circ 20' \text{ W}$	0.5° N	Jan. 1960
Talara, Peru.....	NBS.....	$4^\circ 34' \text{ S}$	$81^\circ 15' \text{ W}$	13° N	Jan. 1960
Baguio, Philippines.	NBS.....	$16^\circ 25' \text{ N}$	$120^\circ 36' \text{ E}$	17° N	Feb. 1960

2. Calculation of the Electron Density Data

For the data discussed here, the well known matrix method of Budden [1955] has been used to derive the electron density profiles. It is unnecessary to review here the details of the primary virtual height-to-true height conversion, since in most respects the procedure has corresponded exactly to Budden's. However, it should be observed that this method has several shortcomings which lead to errors in the $N(h)$ data.

The shortcomings are nearly as well known as the method itself and do not need detailed discussion here; it suffices to itemize them: (a) The electron density is assumed to be a monotonic function of height; if a valley exists there will be a height error which diminishes from a value equal to the valley width just above the valley, to smaller values at greater frequencies. (b) The shape of the profile is somewhat inaccurately determined in regions of strong curvature, because of a convenient but inappropriate assumption made about the variation of electron density within small intervals [Paul, 1960]. (c) Because the ionogram observations themselves do not ordinarily contain information about electron densities below about $10^4/\text{cm}^3$, there is usually an error at night due to neglect of retardation in this ionization.

While one or more of these may be serious for individual profiles, and while their resultant may give mean profile parameters which contain net errors of perhaps 10 percent, these errors are small compared with the total variations discussed here and should not invalidate our conclusions.

The result of the primary matrix multiplication is a table of true heights at particular plasma frequencies. It is more convenient to derive from these data certain other quantities amenable to convenient physical interpretation. Our primary true height data has therefore been put through a secondary calculation process in which the following parameters are derived:

2.1. Electron Density at Fixed Heights

The plasma frequencies (f_N) are converted to electron densities by the relation $N(\text{electrons}/\text{cm}^3) = 12,400 f_N^2 (\text{Mc/s})^2$. A linear interpolation among the corresponding true heights then provides the electron density at 10 km height intervals throughout the observable portion of the profile.

2.2. Height and Characteristic Thickness at the F_2 Peak

Ionograms contain no direct information from a layer peak itself, since the virtual height of a radio-frequency penetrating just to this level is immeasurable. Nevertheless, this level is of unique interest, and it is essential to devise means for its description. A practical method is to fit the portion of the true height profile near the peak with a suitable curve, and to determine the parameters of the peak from

this curve. The parabola is the simplest curve for this purpose, and has the additional merit of closely approximating the peak of a "Chapman" distribution. The parabola is given by

$$N = N_{\text{max}} \left\{ 1 - \left(\frac{h_{\text{max}} - h}{Y_m} \right)^2 \right\}, \quad (1)$$

where h_{max} is the height of the layer peak, N_{max} the peak electron density corresponding to the critical frequency, and Y_m is a parameter characteristic of the thickness of the layer. This curve has been fit to the highest portion of our true height curves, using the measured critical frequency and two true heights: the highest and the fourth from highest. The accuracy with which the parabola may be fit to these data depends slightly upon the spacing of the two heights and rather critically upon the accuracy of determination of N_{max} . In the data described here, various checks have been applied to eliminate extreme errors due to the latter cause. The frequency spacing of the two true heights used for fitting the parabola is a compromise between a narrow spacing (sensitive to small relative errors in the data) and a wide spacing (sensitive to real departures from the parabola). In practice, these points are separated by about 0.8 Mc/s.

In addition to the height of the peak, the quantity $Y_m/2$, which we call "*Scat*",¹ is determined. This is the quarter-thickness of the parabola, and is taken as a measure of the scale height of the atomic species at the level $h_{\text{max}} F_2$, in what follows. The reasons for this interpretation are given briefly in the following section.

2.3 Extrapolation of Profiles Above $h_{\text{max}} F_2$

For sunspot maximum conditions it was previously shown [Wright, 1960] that an electron distribution above the F_2 peak of the form

$$N = N_{\text{max}} \exp \frac{1}{2} \left\{ 1 - \frac{h_{\text{max}} - h}{H} - \exp \left(- \frac{h_{\text{max}} - h}{H} \right) \right\} \quad (2)$$

agreed fairly well with available rocket and other data, for a neutral particle scale height of $H=100$ km. This is, of course, the well-known equation derived by Chapman for the equilibrium distribution due to electron production and recombination-type loss, but it is also the equilibrium form theoretically expected of a layer under the combined influences of diffusion and attachment-like loss, as has been shown by Hirono [1955], among others. Since these latter processes are thought to be effective in determining the F_2 peak [Ratcliffe et al., 1956], the use of eq (2) for extrapolation above the F_2 peak has some theoretical justification. Since eq (2) approxi-

¹ The terms *Scat*, *Shmax*, *Shinf* have evolved in our $N(h)$ system as short pronounceable names for Scale Height, "*f* to h_{max} " and "*f* to h_{∞} ", respectively.

mates to the parabola of eq (1) with $Ym=2H$, the interpretation of *Scat* in terms of the scale height receives a similar degree of theoretical justification.

Each of the hourly profiles used in this study has been extrapolated above $h_{max}F2$ by eq (2), with $H=100$ km. The total electron content, which we term *Shinf*, is given by adding to the subpeak content *Shmax* (vide infra), the quantity $2.82H N_{max}$, as may be shown easily by integration of (2) between limits h_{max} and infinity.

2.4. Subpeak Electron Content

The total number of electrons in a unit column extending from the lowest observable ionization (usually about $10^4/cm^3$) to h_{max} , is termed *Shmax*. It has been obtained in the course of our secondary calculations by numerical integration of the profiles between these two limits.

2.5. Mean Electron Density Profile Data

The systematic calculation of hourly profiles provides a great quantity of data containing, among other inhomogeneities, various degrees of ionospheric disturbance. Our first objective has been to derive mean quiet conditions from these data. This has been done by eliminating profiles at those hours for which the magnetic character figure *Kp* exceeds 4; from the remaining data, the monthly mean values of electron density at 10 km height intervals, and similar averages of the other special quantities are obtained for each hour. Generally, data from about 20 profiles comprise such a mean.

At the same time, the standard deviation of the data entering each mean is obtained. For some of the parameters, a more useful measure of the variability is the relative standard deviation or percentage variability of the quantity. This is obtained by dividing the standard deviation by the mean. From the program described here, the behavior of $(\sigma h_{max})/h_{max}$, $(\sigma Scat)/Scat$, $(\sigma Sh_{max})/Sh_{max}$, and $(\sigma N_{max})/N_{max}$ is discussed in an appendix to this paper.

3. Typical Examples of TN 40—Series Representations

The mean values of the quiet-day electron density profiles and their derived parameters, for each month of the year March 1959–February 1960, are portrayed in a variety of representations in the NBS Technical Note series 40–1, 2, 3, . . . etc. Typical diagrams from this series will first be illustrated and discussed here, as an introduction to the parameters and as a brief review of the variety of information available. While comments are offered regarding the significance and interpretation of specific phenomena evident in these diagrams, no attempt is made here to discuss the generality of the phenomena; rather, the aim is to point out several of the special properties of each form of representation. Throughout, it should be borne in mind that our data and conclusions pertain to a period near the maximum of the solar cycle. In the following

sections the entire body of data will then be represented in a series of month-by-hour diagrams (for a year running from May 1959 through April 1960), which summarize the diurnal and seasonal variations in the northern mid-latitude ionosphere.

3.1. Vertical Cross Sections

Figure 1 (from NBS Tech. Note 40–6) illustrates a vertical cross section of the ionosphere, nominally above the 75° W meridian between geographic latitudes of 15° and 50° N, for 1700 75° W time, August 1959. Contours of plasma frequency f_N in Mc/s, related to electron density N by $12,400 f_N^2 = N$ electron/cm³, represent the true heights of reflection of vertically incident radio waves. The height of maximum electron density is represented by the dashed line, and electron densities above this level are the result of an extrapolation according to the model discussed in section 2.3. Lines of the geomagnetic field would be very nearly vertical within this diagram, and are therefore omitted. Note that the vertical scale is expanded relative to the horizontal by a factor of about 5.5.

Near the level of maximum density a latitudinal gradient of about 0.0015 Mc/s per kilometer or 0.16 Mc/s per degree of latitude may be seen, and this is a fairly typical maximum value at this latitude. It becomes rapidly smaller at heights below the maximum, and not so rapidly smaller at heights above the maximum. It is interesting to note that the latitu-

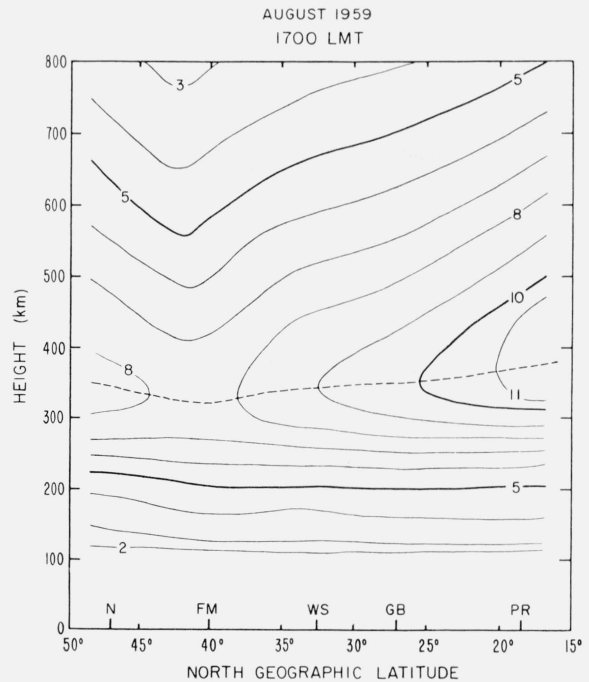


FIGURE 1. Vertical cross section along 75° W meridian. Contours of plasma frequency in Mc/s.

Dashed line represents height of F2 peak. Contours above this level obtained from Chapman model with $H=100$ km.

dinal gradient considerably exceeds the longitudinal sunrise gradient. A typical value of the sunrise gradient is 0.0007 Mc/s per kilometer or 0.07 Mc/s per degree of longitude near the F_2 layer maximum.

3.2. Electron Density Maps in Latitude Versus Time

Contours of electron density at constant heights of 200 and 300 km are shown in figures 2 and 3, for the months June 1959 and January 1960, respectively. In these diagrams, the contours are given at intervals of 10^5 electrons/cm³. In addition to illustrating the diurnal variation of electron density at a fixed height versus latitude, these diagrams may also be considered as representing the mean longitudinal variations when it is noon over the 75°W meridian. For this purpose, the latitude scale is expanded by a factor of 10.76 relative to the "longitude" (time) scale.

At 200 km (fig. 2), the almost exclusively solar control of the ionization densities is obvious: the electron densities rise rapidly at sunrise from values less than 10^4 /cm³ (the minimum detectable with ordinary observing devices) and decrease below this limit a little more slowly at sunset. A small latitudinal gradient may be seen corresponding to the greater solar zenith angles nearer the equator. Note, however, that at this season one of the anomalies of the ionosphere at higher altitudes is reversed at 200 km: the maximum electron density is reached *before* noon, at least at the higher latitudes. This diurnal asymmetry has been noted by Croom et al. [1959].

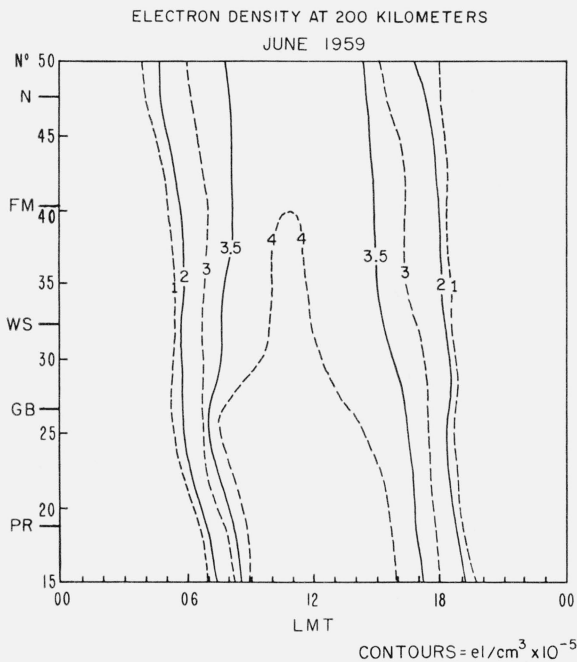


FIGURE 2. Latitude versus local-time isoionic map at 200 km. Contours in electrons per cm³ × 10⁻⁵.

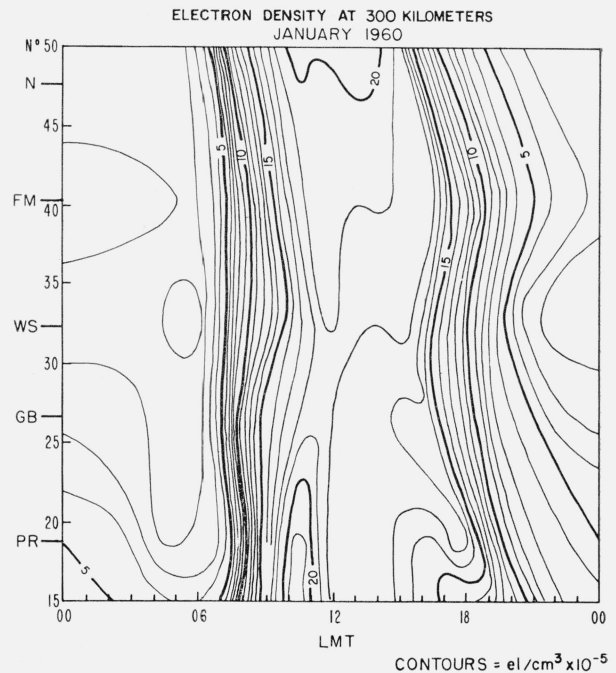


FIGURE 3. Latitude versus local-time isoionic map at 300 km. Contours in electrons per cm³ × 10⁻⁵.

At 300 km (fig. 3) strong solar control is also evident, but it is clear that other factors are relatively more important than at lower altitudes. The initial increase of electron density at sunrise is nearly the same at all latitudes, although the later midmorning values are considerably greater at low latitudes. There is also a peak above 45° N, which is partially explained by the lower altitude of the entire layer there. The curious irregularity in the midday contours, which appears to "move" to later hours at lower latitudes is explained by the latitude/time variations of the height of maximum density: $h_{max}F_2$ is nearly 300 km and varies with time above and below 300 km in the vicinity of this irregularity.

3.3. Latitude Versus Time Variation of $h_{max}F_2$

The height of the F_2 peak is illustrated for March 1959, in figure 4. This is one of the simplest of similar diagrams for other months. Its most obvious feature is that the F_2 peak falls at sunrise from about 380 km to about 300 km uniformly at all latitudes. The daytime variation is characterized by a gradual rise at all latitudes, but this proceeds more rapidly, and reaches a higher daytime altitude, at the lower latitudes. It continues to increase until sunrise at middle and higher latitudes, but decreases somewhat before midnight at low latitudes.

3.4. Latitude Versus Time Variation of F_2 Layer Thickness

The "thickness" of the F region is characterized by our quantity "Scat," the quarter-thickness of a

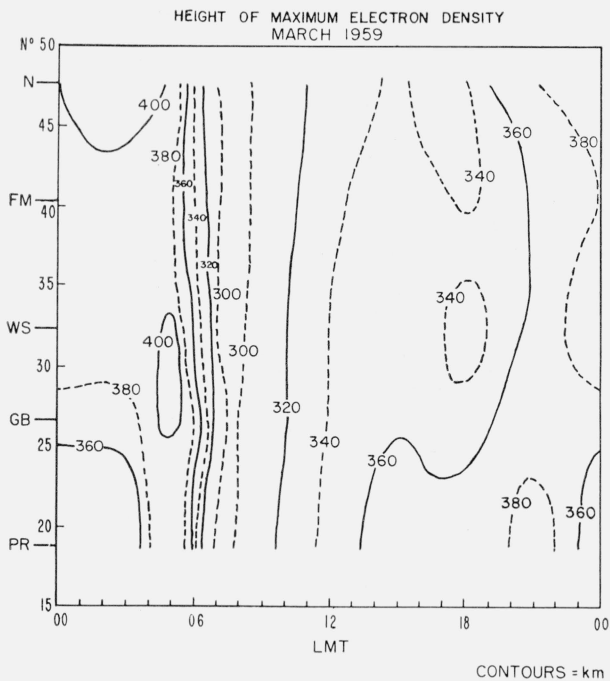


FIGURE 4. Latitude versus local-time map of the height of the F_2 peak.
Contours in kilometers.

parabola fit to the F_2 peak. Its latitudinal and time variations are illustrated in figure 5 for the month of July 1959. This parameter is of special interest since it is probably an approximate measure of the neutral particle scale height—and hence the temperature—at the F_2 peak. It is at once clear that the thickness is strongly under solar control, increasing at sunrise from a nighttime value of about 50 km to about 70 km during daytime. In a significant departure from solar control, however, the higher latitudes have a thicker daytime F region than the lower latitudes.

3.5. Latitude Versus Time Variations of Sub-Peak Electron Content

The number of electrons in a unit column below the F_2 peak is designated Sh_{max} ; its latitudinal versus time variations for May 1959 are illustrated in figure 6. The behavior of the electron content is extremely simple, closely following the solar zenith angle. Nevertheless, certain anomalies are evident. At low latitudes, the maximum value of Sh_{max} follows noon by $1\frac{1}{2}$ –2 hours, rather in accord with simple theory, while in middle latitudes, the maximum is distinctly at noon. It appears that at higher latitudes the maximum again shifts to post-noon. Also the latitudinal midday gradient in Sh_{max} is very much larger than would be expected from the latitudinal change in midday solar zenith angle.

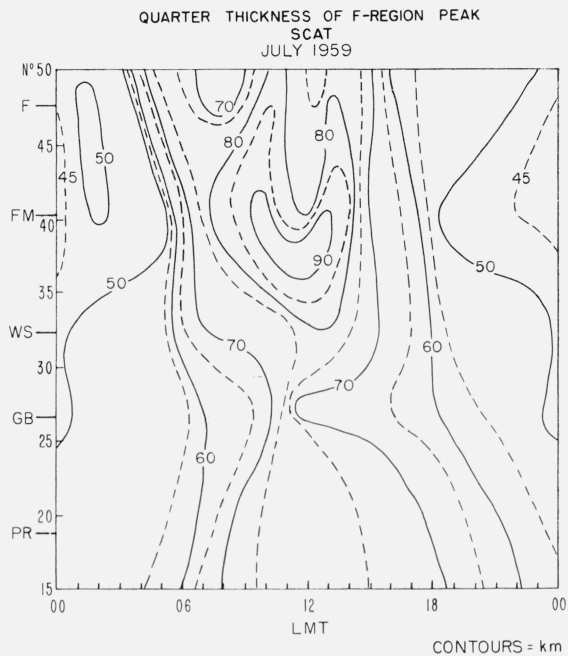


FIGURE 5. Latitude versus local-time map of the quarter-thickness of the F_2 peak.
Contours in kilometers.

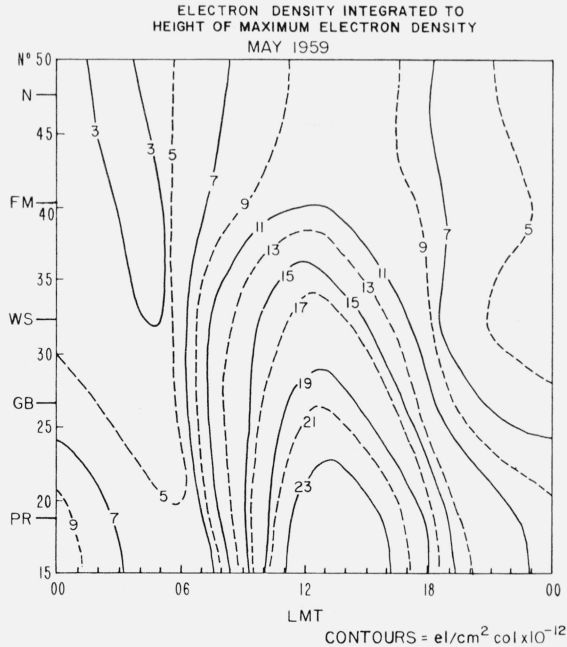


FIGURE 6. Latitude versus local-time map of the subpeak electron content.
Contours in electrons per cm^2 column $\times 10^{-12}$.

3.6. Diurnal Variation of Electron Density at Fixed Heights

The diurnal variation of electron density at a given height is at first sight the most natural representation of ionospheric variations. An example is shown in figure 7, for Puerto Rico, April 1959. When the height of maximum falls below the fixed heights represented here, the corresponding curves are dashed. Such electron densities are the result of the topside model discussed above. The envelope of these curves corresponds to the variation of the maximum density.

It is interesting to note the progressive departure from simple solar control at successively greater altitudes. While the sunrise period (and until 1000) is characterized by a rapid increase of electron density at all heights, there then occurs a general decrease, most marked at heights above 250 km. That at least part of this behavior might be attributable to movement of the layer, is suggested by the post-sunset *increases* in electron density which occur at successively later times at lower altitudes.

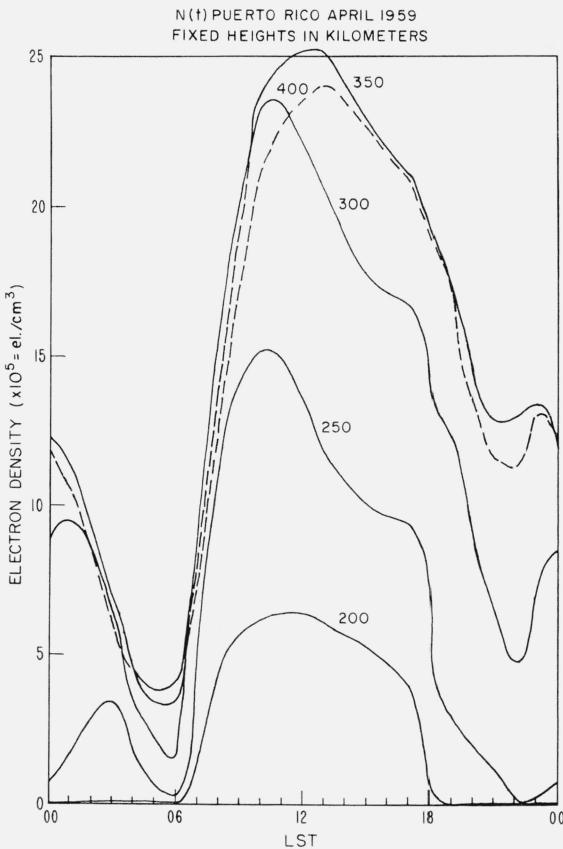


FIGURE 7. Diurnal variation of electron density at fixed heights. Contours in kilometers.

4. Diurnal and Seasonal Variations

A great deal of the basic information describing the F region of the ionosphere is contained in the parameters $h_{max}F$, $Scat$, N_{max} , and Sh_{max} , which measure the height, thickness, and electron density at the peak, and the sub-peak electron content, respectively. These parameters have been displayed for separate months in the latitude-local time plane, in the NBS Technical Note Series 40; examples of them have been discussed above.

With one year of data available, it becomes practical to display this large quantity of information in very compact form. For each of these four parameters, and each of the five stations, we have prepared contour "maps" showing the diurnal versus seasonal variation of these parameters. Figures 8 through 11 may be referred to in the discussion which follows.

We shall first discuss the various parameters individually from a phenomenological point of view, drawing attention to their characteristic diurnal and seasonal features and to the latitude variation evident from the five stations' data. A synthesis and interpretation is then attempted in section 5.

4.1. Height of the $F2$ Peak ($h_{max}F2$, fig. 8)

Characteristically, $h_{max}F2$ is lowest at the time immediately following sunrise, as low as 250 km in the winter and at higher latitudes. It rises throughout the daylight period and generally continues to rise after sunset and throughout the nighttime period. The total diurnal excursion of $h_{max}F2$ is surprisingly constant (100 km), whatever the season or latitude, except that at midlatitudes the variation is somewhat less in winter. There is a distinct similarity between the daytime 300 km contours at the station pairs White Sands/Grand Bahama, and Fort Monmouth/Newfoundland. These pairs of stations have nearly the same magnetic dip (60° and 72° , respectively), although their geographic latitudes are rather dissimilar.

The largest values of $h_{max}F2$ occur in the summer nighttime, and are typically 400 km. At all but the lowest latitude studied, these high values are centered on local midnight; at Puerto Rico, they occur before midnight, centered on 2100 local time in the summer months. It is interesting to note that this tendency is entirely absent at Grand Bahama, which is farther north by only 8° (geographic, geomagnetic, or dip). On the other hand, the daytime similarity noted above between stations with similar magnetic dip, is also evident in the diurnal/seasonal patterns of the nighttime 400 km contour.

4.2. Quarter-Thickness of the $F2$ Peak ($Scat$, fig. 9)

The possibility of interpreting this quantity in terms of the (neutral particle) scale height at the $F2$ peak (see section 2.3) suggests that $Scat$ may be an important indicator of the temperature in the F region. We shall keep this possibility in mind, as the phenomenology of $Scat$ is discussed.

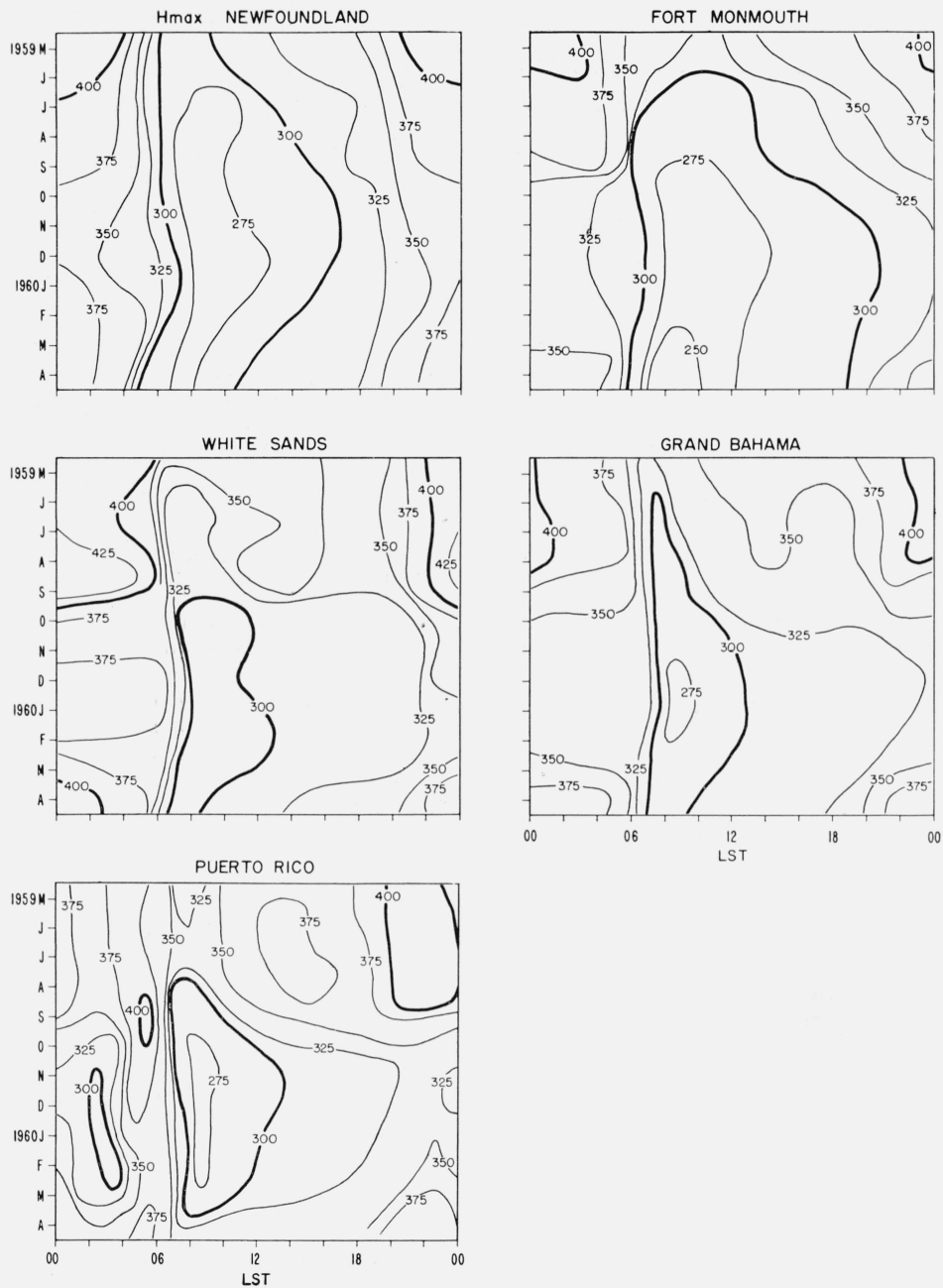


FIGURE 8. Diurnal and seasonal variations of h_{max} .
Contours in km.

Scat shows a diurnal variation at all latitudes and seasons, and this is most marked in the high latitude summer. Noon values of *Scat* approach 100 km in the high latitude summer, but the nighttime values are more typically 50 km or less. At Newfoundland, the highest latitude, the sense of the diurnal variation is reversed in the winter: maximum values then occur in the pre-dawn hours, and generally occur earlier in the equinox months than at the winter solstice. At all other latitudes, the daytime values are distinctly

larger than at night. As with $h_{max}F_2$ there is somewhat more similarity between stations of similar magnetic dip, than among those of similar geographic latitude.

There is a smaller seasonal variation at the lowest latitude (Puerto Rico), with minimum values in the winter and maximum in the summer. The total change is less than at high latitudes, but the smallest values (30 km, winter pre-dawn) are as small as the minima elsewhere.

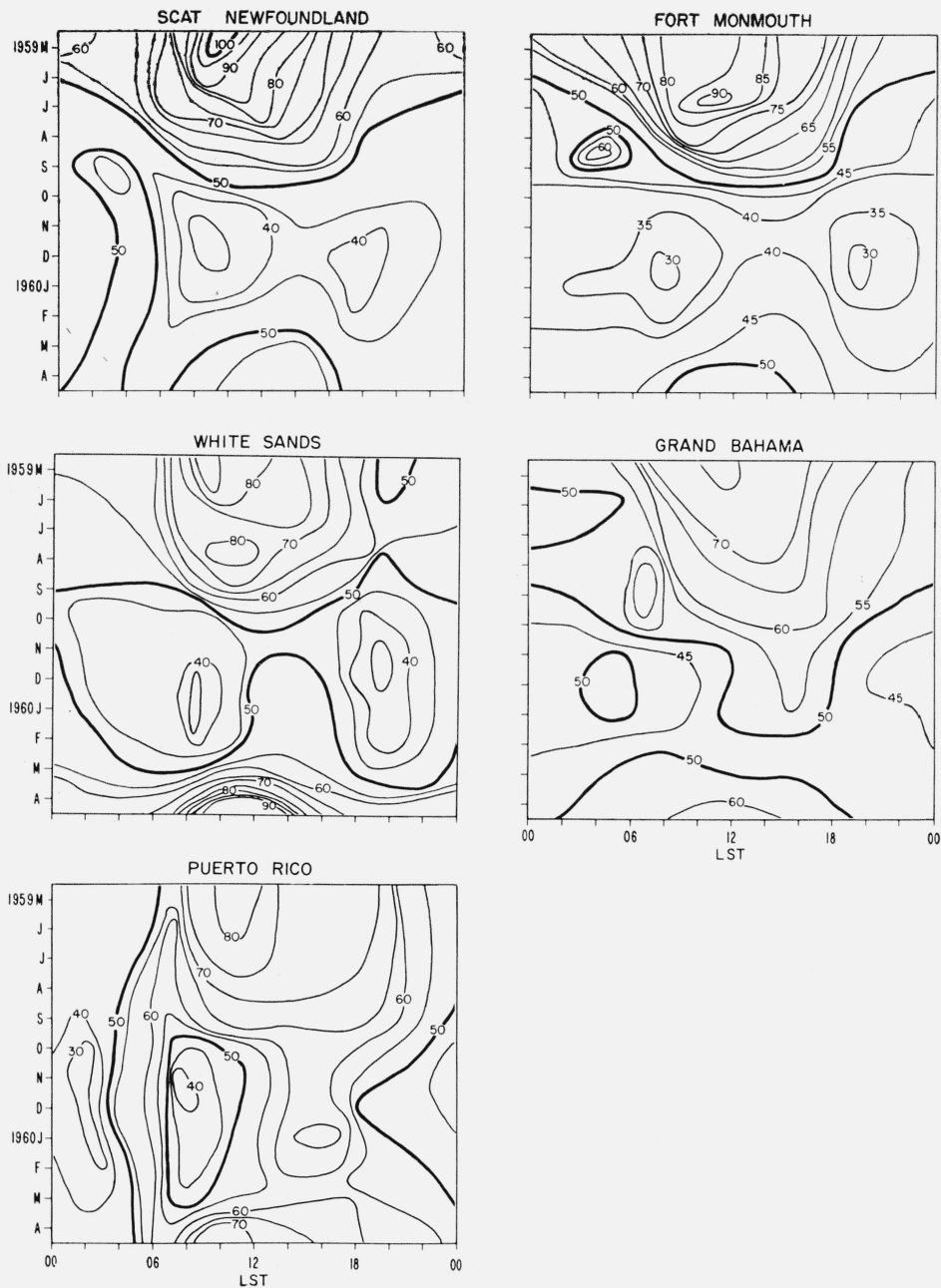


FIGURE 9. Diurnal and seasonal variations of Scat.
Contours in km.

There is a suggestion of a semi-diurnal variation in midlatitude winter, with maxima at 0200 and 1400, minima at 0730 and 1930.

4.3. F_2 Maximum Electron Density ($N_{max}F_2$, fig. 10)

Although the phenomenology of this parameter is

well-known from its direct relationship with foF_2 , we shall review its phenomenology here in order to complete our picture of variations at the F_2 peak. It will also prove interesting to compare $N_{max}F_2$ with the F_2 subpeak electron content. The very great range of $N_{max}F_2$ (through a factor of ten at all latitudes) renders the maxima very prominent, and the minima only slightly less so.

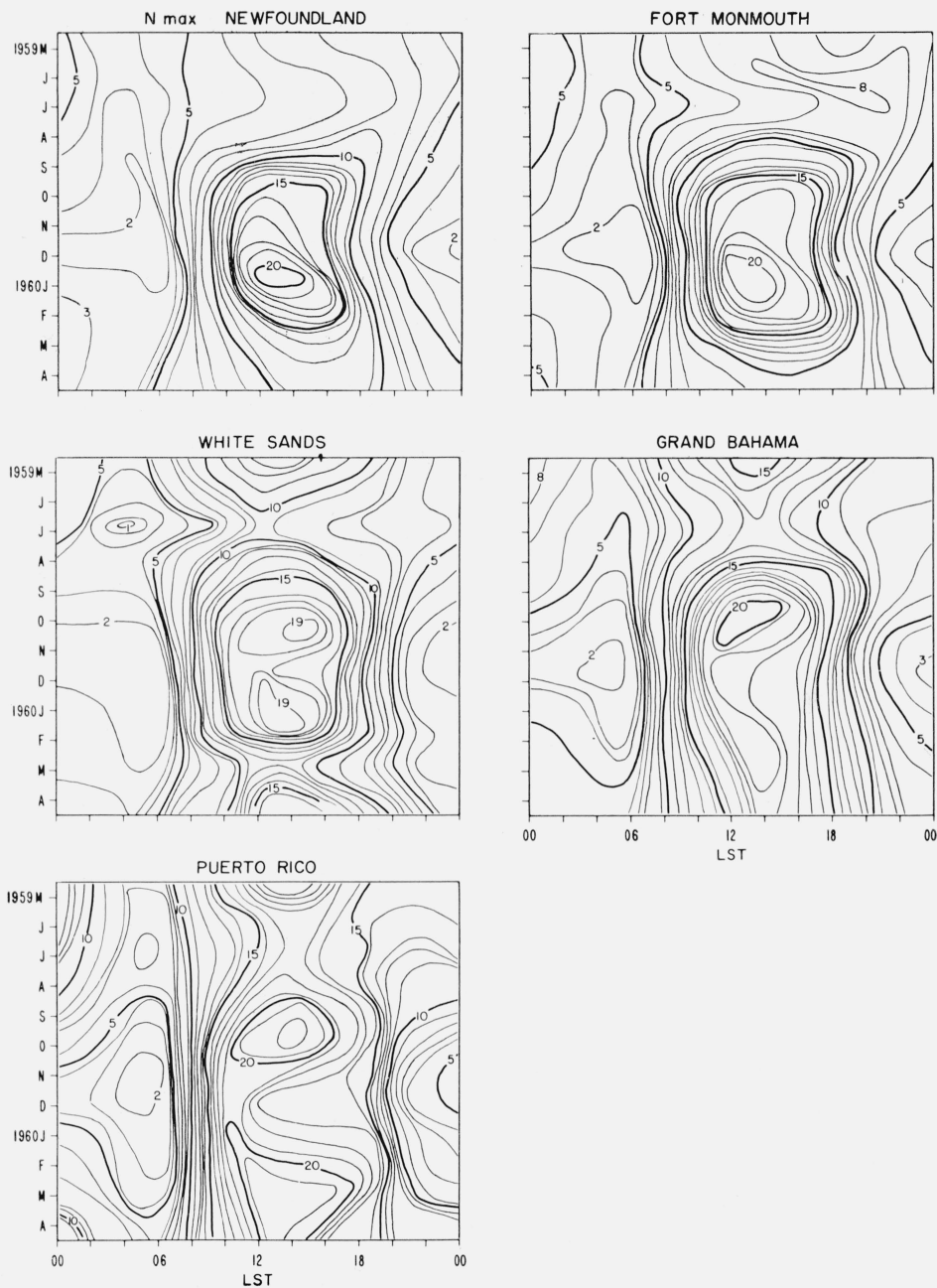


FIGURE 10. Diurnal and seasonal variations of $N_{max}F_2$.
Contours in $(\text{electrons}/\text{cm}^3) \times 10^{-5}$.

In the daytime, high latitudes show a single winter post-noon maximum, which shifts wildly to late afternoon in summer, while at lower latitudes the post-noon maximum is between 1300–1400, nearly independent of latitude or season. The similarity between the late afternoon summer maxima at Ft. Monmouth and Newfoundland suggests magnetic rather than solar control for this anomaly.

Low latitudes show distinct equinoctial maxima, with minima in the summer and winter. At intermediate latitudes, the daytime seasonal variation is complicated by the transition between these two clear patterns. The equinox noon maxima at low latitude provide the very highest values of N_{max} . At higher latitudes, the highest values are nearly independent of latitude, but possess the diurnal and seasonal pattern just mentioned.

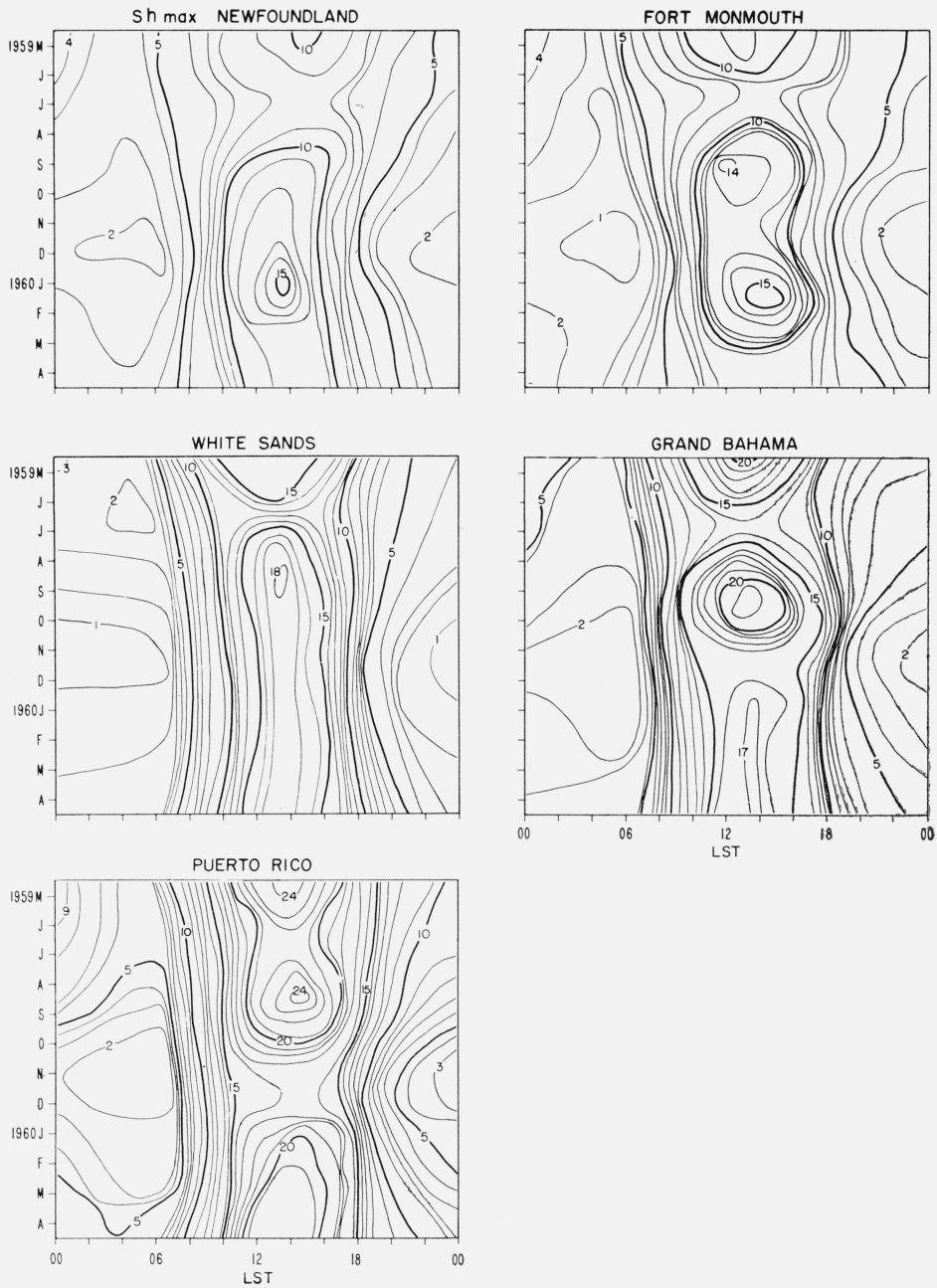


FIGURE 11. Diurnal and seasonal variations of Sh_{max} .
Contours in $(\text{electrons}/\text{cm}^2 \text{ col}) \times 10^{-12}$.

At night, the minimum values always occur in winter, and the largest values occur in summer, at all latitudes. The minimum value of N_{max} is nearly the same at all latitudes, and occurs in the pre-dawn hours. The period of time occupied by the minimum (seasonally centered on December and diurnally centered on about 0500), becomes larger with increasing latitude.

4.4. Subpeak Electron Content (Sh_{max} , fig. 11)

The detailed variations of Sh_{max} show the influence of each of the preceding parameters. Again considering first the daytime periods, it is clear that the pattern of the maxima is the same as for N_{max} : high latitudes display a winter maximum which

“divides” into two equinoctial maxima at lower latitudes. The maxima are generally post noon, but not as late as those of N_{max} . The pre-noon increase in Sh_{max} is more uniform with season and with latitude than is the case with N_{max} . The maximum values of Sh_{max} decrease with increasing latitudes.

At night, the minimum values of Sh_{max} occur in the pre-dawn period, and are lowest in winter. However, there is a tendency, also suggested in the N_{max} data, for the lowest values to occur *before* the winter solstice, rather than at it. The minimum values of Sh_{max} decrease with increasing latitude.

5. Normal Conditions in the F Region; the Seasonal Anomaly

An understanding or interpretation of the complicated behavior of the F region, as illustrated above, is handicapped from the start by the fact that no single influence appears to exert dominance in a consistent way. While solar radiation is obviously the ultimate influence, it is well known that the elementary Chapman theory of ionospheric layer formation predicts that the maximum electron density should vary as $(\cos \chi)^{\frac{1}{2}}$, and it is equally well known that the $F2$ layer does not obey this law. However, Ratcliffe [1951] observed that somewhat

better correspondence with this law was obtained if one used, instead of N_{max} , the subpeak electron content Sh_{max} .

Seasonally, one of the anomalies of the $F2$ layer is that $N_{max}F2$ is greater in winter than in summer, quite in contradiction of simple theory. This has been illustrated already in the discussion of the diurnal and seasonal patterns of $N_{max}F2$ (section 4.3). Ratcliffe's [1951] data suggested that this anomaly was not present in Sh_{max} , and his conclusion was supported (but imperfectly) by Osborne [1952]. We should now like to demonstrate that the $\cos \chi$ variation of Sh_{max} is indeed more regular than that of N_{max} , but that a seasonal anomaly persists in Sh_{max} in mid and higher latitudes. Furthermore, our data show that it is the summer which should be considered anomalous.

Consider the lower portions of figure 12. The mean quiet values of N_{max} between the hours of sunrise and noon are plotted logarithmically versus $\cos \chi$ for the year's data, May 1959–April 1960, for the two stations Newfoundland and Puerto Rico. Summer values are shown by X's, winter values by open circles, and equinox values by filled circles. The seasonal anomaly mentioned above is evident in the considerable extent to which the winter values of N_{max} exceed those in summer. The anomaly is less marked at Puerto Rico than at Newfoundland.

On the other hand, consider the upper part of this figure. Here, the corresponding variations of Sh_{max}

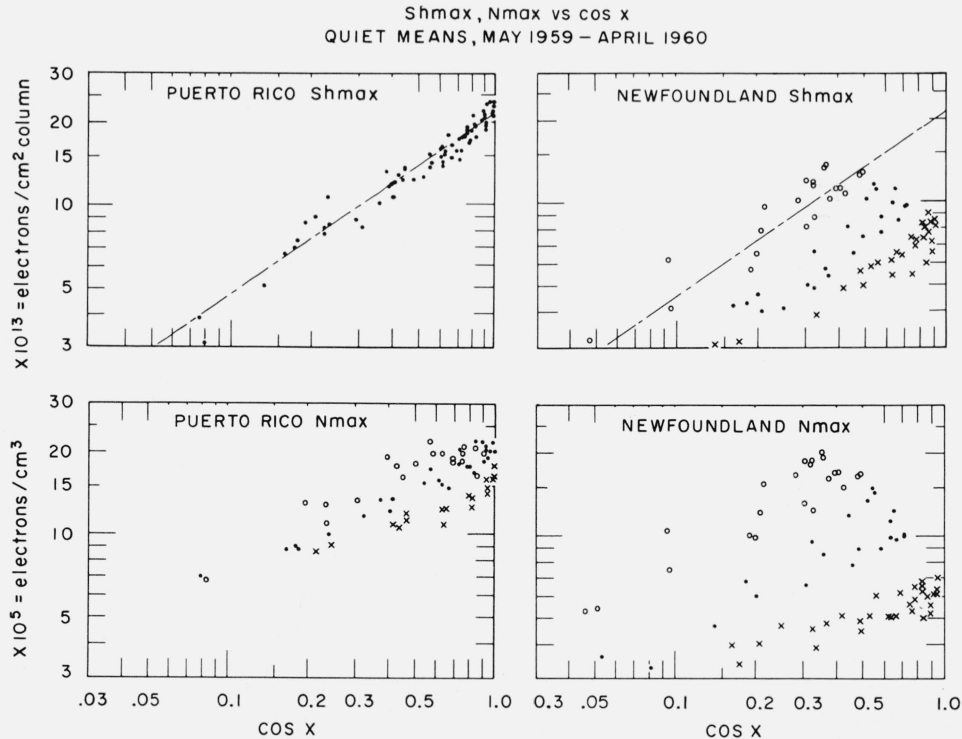


FIGURE 12. Variation of Sh_{max} (upper portion) and N_{max} (lower portion) versus $\cos \chi$, between hours of sunrise and noon at Newfoundland and Puerto Rico.

Key: winter values \circ , equinox values \bullet , summer values \times ; no distinction made for Puerto Rico Sh_{max} .

versus $\cos \chi$ are shown for the same stations. It is at once apparent that the seasonal anomaly is entirely absent at Puerto Rico, but easily detectable at Newfoundland. At the higher latitude it is, however, distinctly less well marked than in N_{\max} .

Stations at intermediate latitudes (Grand Bahama, White Sands, and Fort Monmouth) were examined in a similar way, and found to behave in a manner intermediate between the extremes shown here, in correspondence with latitude.

The line passing through the Puerto Rico Sh_{\max} versus $\cos \chi$ data is also drawn on the corresponding graph for Newfoundland, and it is seen that it agrees reasonably well with the winter points. This same agreement is found with the winter data at the intermediate stations mentioned above. Therefore, it appears that it is the *summer* season which is anomalous, and that in the winter time the subpeak content of the ionosphere approximately obeys the Chapman Law at all latitudes. It is remarkable that at the latitude of Puerto Rico, this same law is obeyed at all seasons. The line in this figure is given by $Sh_{\max} = 2.2 \times 10^{13} (\cos \chi)^{0.68}$ electrons per cm^2 column. In this one regularity of the subpeak electron content, it appears that we have an important clue to some of the causes of the otherwise puzzling behavior of the F region.

6. A Synthesis and Partial Interpretation of the Preceding Observations

6.1. Assumptions

It would be quite difficult, and perhaps impossible at this point, to give a quantitative explanation for all the features of the mean quiet ionosphere portrayed in the preceding figures. However, a qualitative discussion is certainly useful, since the various factors to be mentioned must at least account qualitatively for these data before quantitative tests can be devised. We shall therefore attempt to construct an argument which can account qualitatively for most of the behavior described above. At the outset, several assumed conditions and relationships should be stated:

(1) It is assumed that the main features of figures 8–11 are representative of the real ionosphere, and are not seriously influenced by errors in the calculation of the individual $N(h)$ profiles.

(2) The calculated F_2 layer quarter-thicknesses ($Scat$) are taken to indicate the variations in neutral particle scale height at the level of the F_2 peak as discussed in section 2.3.

(3) Thermal equilibrium is assumed, and therefore the variations in $Scat$ are taken as indications of the temperature variations of the neutral atomic and molecular species at the level of the F_2 peak.

(4) The height of the F_2 peak is presumed to be influenced most strongly by diffusion, balanced by an attachment-like loss process [Ratcliffe, 1960, p. 440].

(5) The attachment-like loss process has an effective attachment coefficient assumed to be of

the form $\beta = \beta_0 \exp \{-(h-h_0)/H_{xy}\}$, where H_{xy} is the scale height of the molecular species involved in the ion-molecular charge exchange process, probably molecular oxygen [Ratcliffe, 1960, p. 383].

6.2. Diurnal and Seasonal Temperature Variations at the F_2 Peak

By assumption 3 above and the diurnal/seasonal variations of F_2 quarter-thickness discussed in section 4.2, it is evident that large diurnal, seasonal, and latitudinal temperature variations occur at the level of the F_2 peak. It is possible that a small part of this variation may be ascribed to vertical motion of the layer in a region with a height gradient of scale height, but it seems clear that large temperature variations must occur throughout the F_2 layer if the layer thickness is any guide. Other evidence for the diurnal variation has recently been given by Jacchia [1961]; he has described diurnal variations of F region temperature as determined from satellite drag data that are similar to the variations suggested here.

However, the scale height, or temperature variations implied by figure 9 are not attributable solely to solar radiation as the heat source. In fact, the following evidence of two significant sources of heat at the F_2 peak may be seen in figure 9.

(a) Seasonally, diurnally, and latitudinally, the temperature increases with decreasing solar zenith angle, consistent with solar heating of the atmosphere.

(b) Data from the higher latitude stations suggests that corpuscular heating is becoming important above about 70° dip. Evidence for this is the following:

i. Above 70° dip, the summer daytime F_2 thickness is at least 25 percent larger than in similar periods at lower latitudes, despite the smaller zenith angles there. This difference cannot be explained by a gradient of scale height with height, since $h_{\max} F_2$ is slightly lower at higher latitudes.

ii. The minimum nighttime F_2 thickness at the highest latitude is also about 25 percent greater than the corresponding values at lower latitudes. If this were to be explained entirely by the slight difference in nighttime $h_{\max} F_2$ between the two latitudes, it would require an improbably large height gradient of scale height of $dH/dh = 0.5$.

iii. In high latitude winter, the F_2 thickness is larger at night than in the daytime, reaching its diurnal peak in the early morning hours, and at an *earlier* hour in the equinox. This behavior corresponds to the diurnal and seasonal incidence of auroral activity at these latitudes [Harang, 1951].

Thus, these data suggest the following general thermal behavior: at low latitudes the heating of the F_2 region is predominantly solar, and depends primarily on the solar zenith angle. At higher latitudes there is superimposed on the solar heating, an auroral-

zone heating of the $F2$ region that increases all temperatures by roughly 25 percent.

6.3. Effect on the Production and Loss of Ionization

The increases in temperature described above cause increases in the neutral particle density at $F2$ heights. In an atmosphere in diffusive equilibrium containing atoms and molecules of the species 0 and O_2 , an increase in the total density implies an increase in the atomic density that goes as the square root of the increase in the molecular density, if the rate of production of the former from the latter is not altered.²

Since it is believed that the rate of loss in the F region varies as $n(O_2)$ while the rate of production varies as $n(0)$, it can be seen that an increase of temperature increases the loss rate to a greater extent than it permits an increase in the rate of electron production.

6.4. A Qualitative Explanation of the Seasonal Anomaly

a. Daytime

At low latitudes it appears that the electron production and loss processes, even though influenced by diurnally varying temperature, cause a "normal" electron density variation that is approximately Chapman-like in the morning hours at all seasons, although the reasons for this remain to be explained quantitatively. At higher latitudes in the summertime, auroral and solar heating together increase the loss rate over the winter value to such an extent that the overall electron content in daytime is significantly reduced, despite the fact that the electron production rate has increased also. During high latitude winter, the solar heating component is reduced and the remaining auroral heating component is apparently insufficient to destroy completely the "normal" behavior of the F region. It should be noted that it is the summer season during which the $F1$ layer appears.

b. Nighttime

At night, there is no seasonal anomaly: Nighttime densities are smaller in the winter than in the summer and this is true at all latitudes, as may be seen in the N_{max} and Sh_{max} diagrams of figures 10 and 11. At first sight, this may seem inconsistent with the explanation just advanced for the daytime variations. However, consideration of the factors dominant at night shows that this is not so. The nighttime-variations of electron content are explainable in terms of the equilibrium height of the F region affected by combined processes of diffusion and attachment-like electron loss [Duncan, 1956]. By this theory, the nighttime F region peak settles rapidly to an equilibrium height at which the effective attachment coefficient is given by

$$\beta = g \frac{\sin^2 \varphi}{2H\nu} \quad (3)$$

² I am indebted to my colleague R. B. Norton for emphasizing the importance of this.

where g is the gravitational acceleration, H is the scale height of the atomic species at the level in question, ν is the positive ion collisional frequency, and φ is the magnetic dip. We shall call the value of β at this height the "equilibrium value," β_e . At the same time, the electron density distribution approaches the Chapman form

$$N = N_{max} \exp \frac{1}{2}(1 - z - e^{-z})$$

where

$$z = \int_{h_{max}}^h dh/H. \quad (4)$$

These same arguments justify the interpretation of $Scat$ in terms of the scale height H , and provide the basis upon which the extrapolations above h_{max} $F2$ have been made.

Equation (3) indicates that an increase in scale height, or temperature, causes a decrease in the equilibrium value of β_e . The positive ion collisional frequency, which varies directly with the neutral particle density, will also increase contributing to the diminution of the equilibrium value, β_e . At the same time, the values of β existing in the atmosphere are larger for larger H , as explained in paragraph 6.3 above. Two effects therefore follow from the higher summer temperatures: (a) the nighttime F region will be found at a greater equilibrium height such that β has its required smaller value; and (b) the summer nighttime F region will decay at a slow rate corresponding to this smaller value of β , resulting in the maintenance of higher electron densities in summer than in winter. In the h_{max} diagrams of figure 8, the nighttime summer equilibrium heights (at, say, midnight) are seen to be higher than the winter heights, in agreement with this argument.

Referring again to the diurnal/seasonal variations of Sh_{max} in figure 11, it can be seen that the values of Sh_{max} at sunset do not vary greatly with season at any latitude. The faster winter loss rates at the lower equilibrium heights will then rapidly decrease the electron content (and N_{max}), thereby accounting for the lower values of these parameters in winter.

7. Summary

Our examination of one year of mean quiet electron density data between latitudes of 18° N and 47° N has been concerned primarily with the properties of the F region near its peak, together with the subpeak electron content of the layer. We have found that, if the characteristic thickness of the region near the peak is interpreted in terms of the local scale height, and hence in terms of the local temperature, the variations of height, thickness and electron content may be explained qualitatively. Several well known anomalies of the F region are similarly accounted for—the seasonal, diurnal, and latitudinal anomalies. The "winter" anomaly, in particular, is found to be misnamed; the data suggest strongly that it is the summer period which should be considered anomalous for its low electron content. The seasonal temperature variations together with an auroral-zone

heating component suggested by the data, are used to explain this summer anomaly in terms of an increased electron loss rate; it is suggested that the $F1$ layer is similarly explainable. The absence of a summer anomaly at night is found to be explainable by the loss rate at the height of the layer peak: with an increase in temperature the layer seeks a greater height where the loss rate is smaller.

As implied in the introduction, this study has been possible only because of the assistance rendered at the data's primary source, the ionospheric field stations; I wish to express my sincere appreciation for the efforts of the many station scientists involved. The NBS $N(h)$ group led by G. H. Stonehocker, has rendered a service that is second only in chronology. Similarly invaluable has been the programming of the work for NBS' high speed computer by Dr. H. H. Howe. Discussions with the author's colleagues S. Radicella, T. N. Gautier, R. A. Duncan, and R. B. Norton have been most helpful in delineating the ideas offered here.

8. Appendix. A Note on the Day-to-Day Variability of the Ionosphere

As was mentioned earlier in the discussion of the averaging process, the standard deviations (σ) and relative standard deviations (σ/mean) of the profile data are also obtained. These parameters give a quantitative measure of the day-to-day variability of the quiet ionosphere, and permit some interesting conclusions regarding the degree to which various external influences control the ionosphere.

The standard deviation of the (roughly 20) values of h_{max} , Sh_{max} , $Scat$, and N_{max} entering their respective means have been determined hourly for each month of the year May 1959–April 1960. In the case of the electron density parameters Sh_{max} and N_{max} , it is immediately evident that the standard deviations are closely proportional to the mean values themselves, and that a clearer picture of the variability of the quantity is obtained if the standard deviation is expressed in percent of the mean value. This is also meaningful for the quarter-thickness, $Scat$, but has little meaning for h_{max} . Accordingly, our figures and remarks will concern the percentage variability of Sh_{max} , N_{max} and $Scat$, but will deal with the true variability of h_{max} , in kilometers.

From the one-year's data available to this study, it has not proven possible to observe any important seasonal variation in these variability data. There is a slight tendency for winter daytime values to be smaller (especially for N_{max} and H_{max}) than at other times and seasons, but this has not been explored further. It is interesting to note, however, the conclusions of section 5 in which other evidence suggests that winter shows a generally less anomalous behavior than summer.

Because of the relatively minor seasonal dependence of the variability parameters, all months of the year's data have been averaged together for the preparation of the latitude versus local time maps of figures 13, 14, 16, 17. These maps show contours of the true variability of h_{max} (in km) and the percent variability of $Scat$, Sh_{max} , and N_{max} , respectively, between latitudes of 15° N to 50° N, versus 75° W time.

8.1. Variability of h_{max}

As shown in figure 13, h_{max} $F2$ has about twice the variability at night as in the daytime, and is generally larger at lower latitudes. The minimum variability is at midday, but the maximum variability is generally post-midnight—markedly so, at lower latitudes.

8.2. Relative Variability of $Scat$

The percent variability of the $F2$ layer quarter-thickness is shown in figure 14. $Scat$ has been interpreted as a measure of the neutral scale height and hence the temperature at the $F2$ peak throughout this paper. Its variability is generally larger at high latitudes and in the early morning or sunrise periods, ranging from 10 percent to 30 percent of its mean value. The greater variability at high latitudes may be related to the importance of corpuscular heating at latitudes approaching the auroral zones, as proposed in section 6.2; it is reasonable that any corpuscular heating of the atmosphere will have more day-to-day variability than the heating due to solar radiation.

It is of interest to inquire to what extent the variabilities of the height of the $F2$ peak and its characteristic thickness are related. It might be imagined, for example, that all the variability of h_{max} might be accounted for by variability in the thickness of the layer. This would be the case if the layer were essentially fixed in position and merely varied in thickness from day to day. Alternatively, it might be imagined that the whole region "moves" vertically from day to day, producing a variation in h_{max} that is essentially independent of variations in the layer thickness.

To examine this point, in figure 15 we have plotted diurnally the standard deviations (in km) of h_{max} $F2$ and $Scat$ for the entire year's data and for the two stations Newfoundland and Puerto Rico. The shaded area shows in each case the part of the variability of h_{max} which cannot be accounted for directly by the variability in $Scat$, or vice versa.

First, one notes that generally h_{max} varies more than $Scat$, except during high latitude daytime, when the two are essentially the same. There is a great difference between the two at night, indicating that the layer is found at considerably different positions (altitudes) from day to day with comparatively little change in thickness. There is, however, some indication of a correlation between the magnitudes of the two parameters.

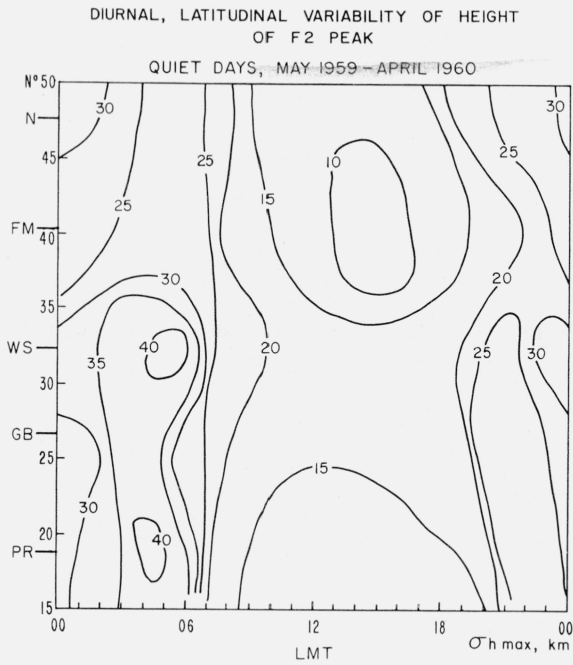


FIGURE 13. Diurnal, latitudinal variability of $h_{\max}F_2$; quiet mean values averaged over May 1959–April 1960; contours in kilometers.

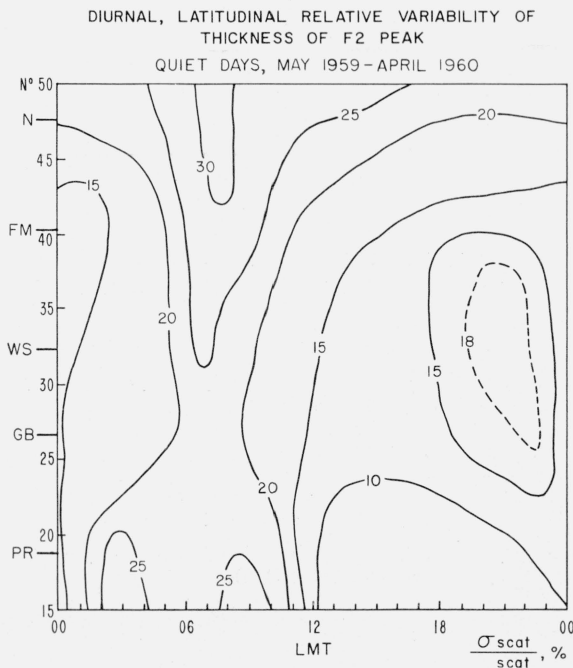


FIGURE 14. Diurnal, latitudinal relative variability of $Scat$; quiet mean values averaged over May 1959–April 1960; contours in percent.

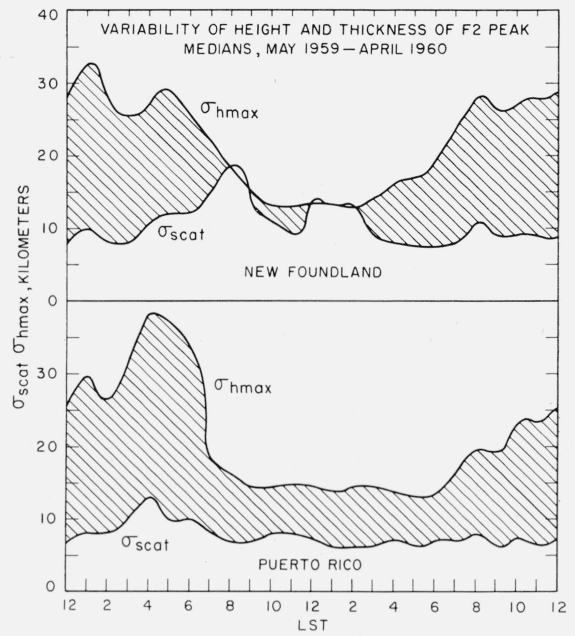


FIGURE 15. Comparative variability of $h_{\max}F_2$ and $Scat$ versus time, at New Foundland and Puerto Rico, averaged over May 1959–April 1960.

8.3. Relative Variability of Total Electron Content

This parameter (fig. 16) has a very regular seasonal and time dependence. It is nearly constant (30%) at night, independent of latitude, and appears to depend very simply upon the solar zenith angle, being smallest during daytime at low latitude. The diurnal minimum value occurs, however, from one to three hours postnoon.

8.4. Relative Variability of Maximum Electron Density

In contrast with the variability of Sh_{\max} , the variability of the maximum electron density (fig. 17) suggests a mixture of latitudinal and solar control. The maximum values (40%) occur in the predawn period at high latitudes. The minimum values occur towards lower latitudes in the daytime, and these become equal to the relative variability in subpeak electron content discussed in paragraph 3. This is consistent with the Chapman-like behavior of the low latitude daytime ionosphere discussed in section 5: If the F region possesses a Chapman-like behavior, the electron density at all altitudes varies in proportion to the maximum density, and hence the electron content does also. This behavior is somewhat evident at all latitudes near midday, but is definitely not the case at night—especially at higher latitudes. However, we may note that the high latitude predawn peak variability of Sh_{\max} occurs at nearly the same time as the peak variability in layer thickness (vide supra). The behavior of the variabilities of N_{\max} , Sh_{\max} , and $Scat$ at high

DIURNAL, LATITUDINAL RELATIVE VARIABILITY OF
SUB PEAK ELECTRON CONTENT

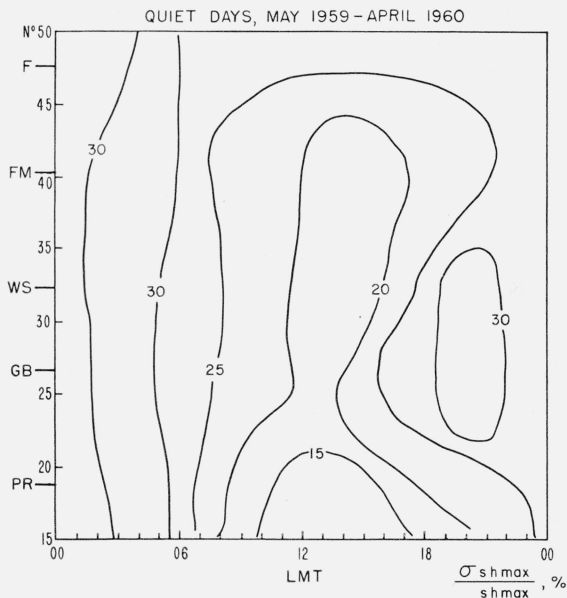


FIGURE 16. Diurnal, latitudinal relative variability of Sh_{max} ; quiet mean values averaged over May 1959–April 1960; contours in percent.

DIURNAL, LATITUDINAL RELATIVE VARIABILITY OF
F2 MAXIMUM ELECTRON DENSITY

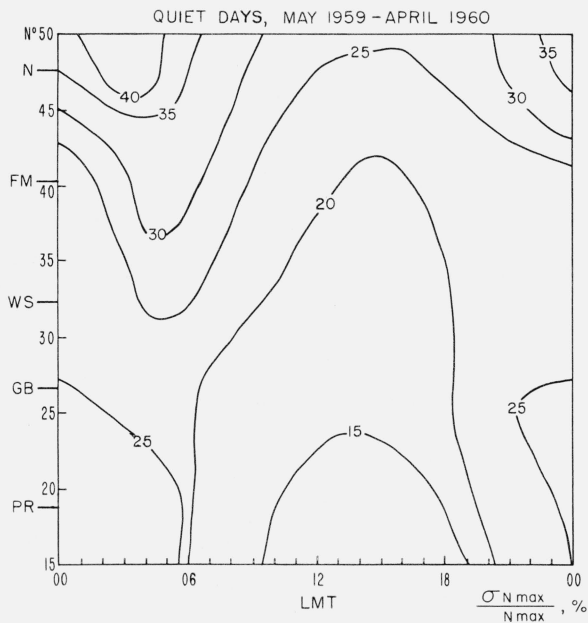


FIGURE 17. Diurnal, latitudinal relative variability of $N_{max}F_2$; quiet mean values averaged over May 1959–April 1960; contours in percent.

latitudes during nighttime are again consistent with the corpuscular heating discussed in section 5.2: As the day-to-day changes in temperature modulate the thickness of the nighttime F region, its maximum density varies in inverse fashion without appreciable change in the electron content.

8.5. Summary

The day-to-day variability of an ionospheric parameter, expressed as a percentage of the monthly mean, has been shown to be subject to interpretation consistent with the physical processes controlling the layer. The variability of a given parameter shows properties relatable to certain physical influences which may be obscured in the real values of the parameters themselves. In particular, the variability of the high latitude nighttime ionosphere is consistent with a variable corpuscular influence (probably heating) not evident at lower latitudes.

9. References

- Budden, K. G., A method for determining the variation of electron density with height ($N(z)$ curves) from curves of equivalent height against frequency ($(h'f)$ curves), from *The Physics of the Ionosphere*, 332–339 (The Physical Society, London, 1955).
- Croom, S., A. Robbins, and J. O. Thomas, Two anomalies in the behavior of the F2 layer of the ionosphere, *Nature* **184**, 2003 (1959).
- Duncan, R. A., The behavior of a Chapman layer in the night F2 region of the ionosphere, under the influence of gravity, diffusion, and attachment, *Australian J. Phys.* **9**, 436–439 (1956).
- Harang, L., *The aurora*, p. 9 (John Wiley & Sons, New York, (1951).
- Hirono, M., Effect of gravity and pressure gradient or vertical drift in the F2 region, *Rep. Iono. Research Japan* **9**, 95 (1955).
- Jacchia, L. G., Irregularities in atmospheric densities deduced from satellite observations, *Ann. Geophys.* **17**, 273 (1961).
- Osborne, B. W., Some practical determinations of electron content below the level of maximum ionization in the F2 region of the ionosphere, *J. Atmospheric and Terrest. Phys.* **3**, 58 (1952).
- Paul, A. K., Bestimmung der wahren aus der scheinbaren reflexionshohe, *Anch. Elekt. Ubertrag.*, **14**, 468 (1960).
- Ratcliffe, J. A., Some regularities in the F2 region of the ionosphere, *J. Geophys. Research* **56**, 487 (1951).
- Ratcliffe, J. A., E. R. Schmerling, C. S. G. K. Setty, and J. O. Thomas, The rates of production and loss of electrons in the F region of the ionosphere, *Phil. Trans. Roy. Soc. A*, **248**, 261 (1956).
- Ratcliffe, J. A. (Editor), *Physics of the upper atmosphere* (Academic Press, 1960).
- Schmerling, E. R., Penn. State Univ. Iono. Res. Lab. Sci. Reports. 105 and 118 (1958–1959).
- Thomas, J. O., The distribution of electrons in the ionosphere, *Proc. IRE* **47**, 162 (1959).
- Wright, J. W., L. A. Fine, L. R. Wescott, and D. J. Brown, Mean electron density variations of the quiet ionosphere, NBS Technical Note 40–1, 2, 3, 4, 5 6, issued to date (1959–1961).
- Wright, J. W., A model of the F region above $h_{max}F_2$, *J. Geophys. Research* **65**, 185 (1960).

(Paper 66D3–198)